How permeable is the edge of the Arctic vortex: Model studies of winter 1999–2000

Hildegard-Maria Steinhorst, Paul Konopka, Gebhard Günther, and Rolf Müller
Institute for Stratospheric Chemistry (ICG-I), Research Center, Jülich, Germany

Received 23 July 2004; revised 12 November 2004; accepted 15 December 2004; published 17 March 2005.

[1] The edge of the Arctic vortex constitutes a strong barrier to transport; however, the extent of isolation of the vortex air as a function of altitude and season is relatively poorly quantified. In this study, by examining the transport of midlatitude air parcels across the vortex edge into the vortex, we analyze the permeability of the vortex edge. With the three-dimensional version of CLaMS (Chemical Lagrangian Model of the Stratosphere) we explore the dilution of the vortex air due to mixing in winter 1999–2000. An artificial, passive tracer was initialized on 1 December 1999 inside the polar vortex with a value of 100% and with a value of zero outside the polar vortex. Using several different definitions of the vortex edge, the resulting intrusions of midlatitude air into the vortex show the same mean features. This demonstrates that the diagnosed dilution does not strongly depend on the details of the definition of the vortex edge. At about the end of March 2000, the vertical structure of the vortex consisted of well-isolated, pure vortex layers around 500 K and 750 K, with some more diluted layers in between and at the vortex bottom. The influence of wave activity on the evolution of the intrusion layers is studied. The divergence of the Eliassen-Palm flux shows such a high variability during the whole period that it is not possible to assess a direct causality of certain intrusion layers and some specific patterns. Some characteristics of the vortex edge, in particular the shape of the gradient of potential vorticity (PV), can influence the dilution of the vortex. In cases without a distinct maximum in the PV gradient, the defined "vortex edge" may vary substantially from day to day. The comparison of some properties of the vortex (wind speed, PV field, area of the vortex, the maximum of the PV gradient) of undisturbed versus diluted layers and the variation in time of the intrusions were analyzed. All observed intrusions begin in conditions of weak PV gradient, indicating that the value of the maximum of the PV gradient may be used as a quantitative measure of the permeability of the vortex edge.

Citation: Steinhorst, H.-M., P. Konopka, G. Günther, and R. Müller (2005), How permeable is the edge of the Arctic vortex: Model studies of winter 1999–2000, *J. Geophys. Res.*, *110*, D06105, doi:10.1029/2004JD005268.

1. Introduction

[2] The polar vortex in winter and spring is surrounded by the polar wind jet. These strong zonal winds act as a kinematic barrier that separates the air within the vortex from the midlatitude air masses [e.g., *Randel et al.*, 1993; *Pierce et al.*, 1994]. Commonly, the vortex edge is identified by the strongest potential vorticity (PV) gradient with respect to equivalent latitude [*Nash et al.*, 1996] and acts as a flexible "eddy-transport barrier" [*McIntyre*, 1995], hindering the transport on isentropes across the vortex edge. An extreme view developed from theoretical arguments and modeling experiments by *Juckes and McIntyre* [1987] considers the polar vortex as a completely isolated "containment vessel." In studies of diabatic descent the assumption of a completely isolated vortex has been employed [e.g., *Rosenfield et al.*, 1994]. Both trajectory calculations [*Manney et al.*, 1994b] and Lagrangian transport studies (trajectory or contour advection) [*Chen*, 1994] indeed show strong barriers to latitudinal mixing above about 420 K and 400 K potential temperature, respectively, throughout the winter, with more mixing below this isentropic surface. Similar conclusions are reported by *Abrams et al.* [1996] for the 1994 Antarctic winter, using ATMOS tracer observations. According to the calculation of isentropic trajectories, in the Arctic winter a strong mixing barrier usually forms near the vortex edge in January and February [*Dahlberg and Bowman*, 1994]. Weaker barriers are found during the months of December and March.

[3] However, the degree of isolation of the polar vortex is not well known [e.g., *Jost et al.*, 2002]. In particular, during its formation in December 1999, midlatitude air can be entrained in the lower stratosphere within the vortex [e.g., *Greenblatt et al.*, 2002]. Their analysis of quite variable balloon profiles (from in situ and remote sensing instruments) and ASUR data (retrieving complete vertical profiles of several gases) in late fall indicated that the polar vortex

0148-0227/05/2004JD005268

was still inhomogeneous at the beginning of December. Similarly, in late December 1996 and early January 1997 the Arctic vortex was not as strongly established as usual; this led to intrusions of midlatitude air masses into the vortex that were diagnosed in N_2O/O_3 relations measured by the ILAS instrument on the ADEOS satellite [*Tilmes et al.*, 2003]. Further, the analysis of PV maps with low PV gradients at the vortex edge in December 1999 [*Newman et al.*, 2002] and the study by *Ray et al.* [2002] support the idea of a weak, inhomogeneous vortex in the lower stratosphere in early December 1999. Above 500 K the vortex circulation is well established by late November [*Kawa et al.*, 2002]. In winter 1999–2000 the Arctic polar vortex was unusually cold in the early winter lower stratosphere [*Manney and Sabutis*, 2000]. Comparing winter 1999–2000 with 21 previous winters, this study shows the complexity and variability of vortex development: despite unusually low temperatures in the lower stratosphere in winter 1999–2000, the lower stratospheric vortex developed more slowly than in previous cold years and was weaker than average until late December [*Manney and Sabutis*, 2000]. *Ray et al.* [2002] compared two models of mixing: constant horizontal entrainment of midlatitude air across the vortex edge and mixing within the vortex, versus an isolated vortex where differential diabatic descent of air masses occurs with subsequent mixing. Changes in tracer profiles can as a first approximation be attributed to descent, except for the bottom of the vortex where mixing with midlatitude air was required, indicating at 400 K that possibly 15–25% of the air in the vortex was entrained from midlatitudes.

[4] From mid-December 1999 to March 2000 the vortex was quite strong and large [*Newman et al.*, 2002]. The extent and distortion of the polar vortex varies from year to year, and is influenced by planetary wave activity [e.g., *Waugh and Randel*, 1999]. With increased planetary wave activities, we also expect increased mixing into the vortex of midlatitude air. Here we carried out high-resolution transport studies with the three-dimensional (3-D) version of the Chemical Lagrangian Model of the Stratosphere (CLaMS) [*McKenna et al.*, 2002; *Konopka et al.*, 2004] from the beginning of December 1999 until mid-March 2000 in order to quantify the vortex dilution over the course of the winter and to trace the mixing across the vortex edge into the vortex to particular dynamical properties of the stratospheric flow. CLaMS is based on a Lagrangian formulation of the tracer transport and a mixing algorithm where the intensity of mixing is driven by the local horizontal strain and vertical shear rates. The parameters controlling the deformation-induced mixing are optimized by finding the best agreement between the simulated distributions of long-lived tracers and high-resolution in situ observations [*Konopka et al.*, 2004, 2005]. In CLaMS, the dilution of the vortex is quantified in terms of an artificial tracer that at the beginning of the simulation (on 1 December) marks the air parcels (APs) inside and outside the vortex by 100 and 0%, respectively. This tracer describes the percentage of the pure vortex air defined in this way in each AP throughout the model run. Using this technique, we show in section 3 that around the end of March 2000, intrusions of midlatitude air into the arctic polar vortex produced a layered vertical structure of the vortex with some "well-isolated" pure vortex air layers and more mixed layers in between. To demonstrate that this structure is independent of the definition of the vortex edge, several criteria defining the vortex edge [*Nash et al.*, 1996; *Tuck et al.*, 2002; *Chan et al.*, 1989; *Konopka et al.*, 2005] were tested. To investigate the dynamical origin of the sharp layer-wise intrusions into the vortex, an analysis of planetary wave activity was carried out both in terms of amplitude and of the Eliassen-Palm flux (see section 2). Whereas we cannot trace all these intrusions to events of enhanced wave activity, we show in section 4 that the steepness of the (modified) PV gradient with respect to the equivalent latitude seems to be a good measure of the permeability of the vortex edge.

2. Wave Activity and Dynamics

[5] Significant amounts of lower latitude air may be mixed into the polar vortex due to disturbed meteorological conditions [e.g., *Dahlberg and Bowman*, 1994; *Rosenfield and Schoeberl*, 2001]. Using the contour advection technique, *Plumb et al.* [1994] describe for winter 1991–1992 three events where there was substantial intrusion of midlatitude air into the vortex. The reality of these intrusions was confirmed by aerosol observations from the lidar aboard the NASA DC-8 and in situ measurements [*Plumb et al.*, 1994]. Analyzing the ozone loss of winter 1991–1992, *Grooß and Müller* [2003] conclude that in January 1992 the major fraction of the change in the vortex average ozone mixing ratio is due to dynamically caused intrusions into the vortex. The degree of mixing in the lower stratosphere depends particularly on the position and evolution of the polar night jet [e.g., *Manney et al.*, 1994b]. Disturbances of the polar night jet can be broadly explained by examining the wave energy propagating out of the troposphere into the stratosphere, with strong wave events decelerating the jet and warming the polar vortex [e.g., *Newman et al.*, 2002]. Wave activity in the stratosphere is driven by forcing of planetary waves from the troposphere. The most important waves propagating into the stratosphere are Rossby waves or planetary waves typically with wave number 1 or 2 [*Schoeberl and Hartmann*, 1991]. Mixing arises from breaking waves. Similarly, experimental observations of fine-scale layering and filamentation in the ozone field between 350 and 400 K were explained by breaking Rossby waves with higher wave numbers [*Bradshaw et al.*, 2002a, 2002b]. Rossby wave "breaking" describing the erosion of the polar vortex [*McIntyre and Palmer*, 1983] reduces the area of the polar vortex [*Butchart and Remsberg*, 1986]. Large wave amplitudes are correlated with large values of the Lyapunov exponent and thus suggest strong mixing [*Schoeberl and Newman*, 1995]. Generally speaking, the Lyapunov exponent is a measure of the deformation of the flow. In CLaMS, where mixing is deformation-induced, the critical Lyapunov exponent is one of the optimized mixing parameters with the highest mixing rates occurring in flow regions with the largest Lyapunov exponents [*Konopka et al.*, 2004b]. We intend to find a parameter which indicates coupling between wave activity, increased values of the Lyapunov exponent, amplified mixing in ClaMS, and intrusions into the vortex. *Nakamura* [2004] presents a method (effective diffusivity) for estimating the permeability of the stratospheric polar vortex. This diagnostic method successfully quantified two-way transport

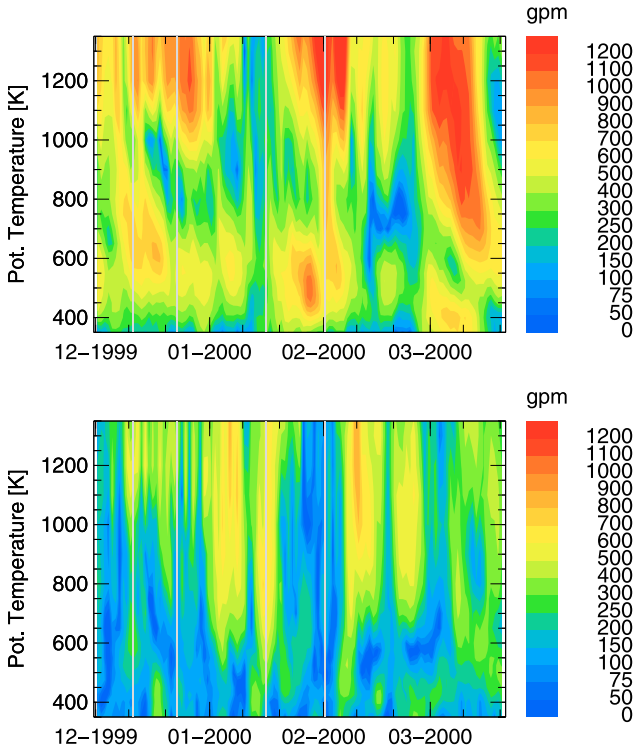

Figure 1. Activity of the planetary waves in winter 1999–2000: amplitude of zonal wave number 1 (top panel) and zonal wave number 2 (bottom panel) in gpm. The vertical gray lines mark the dates of minor warming or wave amplification events (see text for more details).

and hence the direction of wave breaking: the predominantly outward breaking (equatorward) and the rare inward breaking of Rossby waves. Thus, only in the rare cases of inward-breaking waves can midlatitude air parcels cross the vortex edge into the vortex.

[6] Figure 1 illustrates the amplitudes of wave number 1 (top panel) and wave number 2 (bottom panel) using ECMWF data. These findings are in good agreement with the results of *Manney and Sabutis* [2000] and *Sabutis and Manney* [2000]. In particular, in mid-December at 600 K and toward the end of December above 1000 K, strong activity of wave 1 is noticeable. At the end of January and at the beginning of February the activity of wave number 1 increases at all levels. The amplitudes of wave number 2 shows increasing activity in the first half of January and in about mid-January 2000. *Manney and Sabutis* [2000] and *Sabutis and Manney* [2000] studied the evolution of the polar vortex in winter 1999–2000 and reported minor warming or wave amplification events occurring on 11 and 23 December and 16 January. The vertical gray lines in Figure 1 and in Figure 3 in section 3 mark these dates,complemented by an additional warming event on 1 February 2000, as indicated by the extremely high activity of wave number 1 in Figure 1. The minor warming events in December were dominated by wave 1 and the January event by wave 2 activity [*Manney and Sabutis*, 2000].

[7] *Pierce and Fairlie* [1993] determined three preferred flow regimes for the Arctic winter stratosphere from the analysis of the combined frequency distributions of the mean zonal wind and wave number 1 heights during December to February on the 10-mb level. Analyzing 10 years of daily Stratospheric Sounding Unit data from the NOAA satellites, they defined three preferred flow regime modes: mode 1B, with large zonal mean wind velocities ($\geq$27.1 m s^{-1}) and small wave-1 geopotential heights ($\leq$285 gpm), mode 1A, with weak zonal mean wind ($\leq$25.7 m s^{-1}) and weak wave-1 heights ($\leq$285 gpm), and mode 2 regimes, with large wave-1 amplitudes ($\geq$375 gpm). Low mean polar geopotential heights are associated with low polar temperatures. Mode 1B is associated with a deep, cold polar vortex and is characteristic of cold, undisturbed conditions. All anomalously cold winters are associated with persistent mode 1B flow regimes. The mode 1A days show a weak vortex and generally weak gradients of geopotential heights. This mode is associated with major sudden warmings, although it does not appear in all known cases when major warming occurs. Mode 2 days occur most frequently and are characteristic of normal midwinter conditions. *Pawson and Kubitz* [1996] extended the work of *Pierce and Fairlie* [1993] to a 30-year climatology. Using daily FUB data at 10 hPa and 60°N, they isolate the same regimes for the winter stratosphere. On the basis of the empirical distributions of the 30-year data, different boundaries for the flow regime modes were used: mode 1A days are considered to be days with a mean zonal wind $\leq$15 m s^{-1}) and with wave-1 geopotential heights $\leq$600 gpm, mode 1B days with mean zonal wind $\geq$5 m s^{-1}, and wave-1 geopotential heights $\leq$400 gpm, while mode 2 is assumed for large wave-1 amplitudes. Following the categories of *Pierce and Fairlie* [1993], the analysis of the mean zonal wind and geopotential heights at 10 hPa and 60°N for December 1999 to February 2000 yields about 70% mode 2 days and 13% mode 1B days, without any mode 1A days. The missing 17% do not belong to any category. Using the categories defined by *Pawson and Kubitz* [1996] leads to similar results: about 63% mode 2 days and 37% mode 1B days. With this percentage of mode 1B days, winter 1999–2000 ranges among other very cold winters, such as the winter of 1980–1981. The lack of mode 1A days, associated with major warmings, is also consistent with the lack of major warmings in winter 1999–2000. Consequently, our findings regarding mixing into the vortex for winter 1999–2000 indicate a relatively undisturbed vortex.

[8] The divergence of the Eliassen-Palm flux (EP flux) is used as a measure of the zonal mean flow forcing by planetary waves [e.g., *Sabutis and Manney*, 2000]. Breaking of planetary waves has an impact on the mean zonal wind, causing its acceleration or deceleration, and is indicated by non-zero values of the divergence of the EP flux [e.g., *Sabutis and Manney*, 2000; *Rao et al.*, 2003; *Oberheide*, 2000]. Negative values of the EP flux divergence (which are equivalent to convergence) effect deceleration of the zonal wind [*Rao et al.*, 2003]. However, although the EP flux divergence may affect the zonal wind field and thus the polar jet, we are focusing here on intrusions into the vortex, which depend on the strength of the vortex edge, defined by the maximum of wind speed and of the gradient of PV (following the *Nash et al.* [1996] criterion). The strength of the vortex edge is related to the strength of the polar jet, but the relationship between the mean zonal winds and the vortex strength seems to be more indirect. Another way of

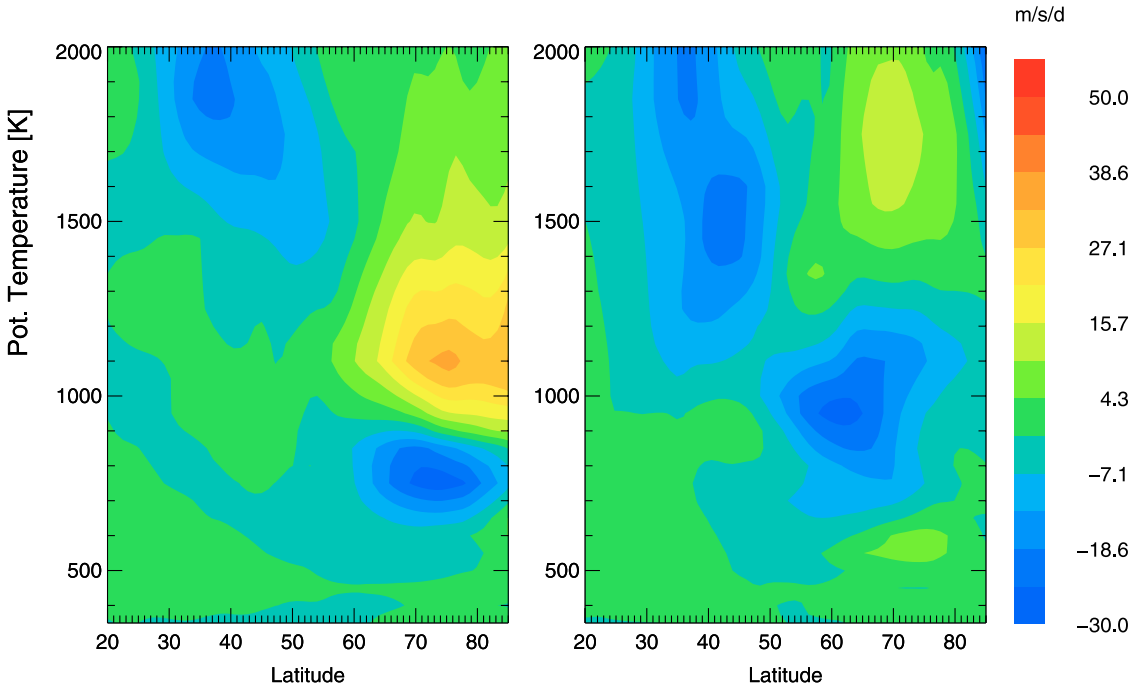

Figure 2. Divergence of Eliassen-Palm flux for enhanced wave activity (23 December 1999, left panel) [*Sabutis and Manney*, 2000] and for ordinary wave activity (3 January 2000, right panel).

measuring the strength of the vortex edge is the PV gradient.

[9] Day-to-day EP flux and its divergence were calculated on isentropic coordinates according to *Andrews et al.* [1987] for θ-levels in the range between 350 and 2000 K potential temperature. For the above-mentioned days with increased wave activity, we find similar EP flux divergences as reported by *Sabutis and Manney* [2000] (e.g., on 23 December 1999; see Figure 2, left panel). However, we find a high day-to-day variability of the EP flux divergence even on days when no significant wave activity was observed (e.g., on 3 January; see Figure 2, right panel). Also, the location of the minima and maxima of EP flux divergence fluctuates intensely from one day to the next, and furthermore in latitude and altitude as well. These rapid fluctuations of the EP flux divergence, reflecting variations in large-scale forcing, did not affect the strength of the vortex edge in any obvious way.

3. Mixing Across the Vortex Edge During Winter 1999–2000

[10] Using an artificial, passive tracer that is transported in CLaMS, we now diagnose the dilution of the vortex air during winter 1999–2000 caused by intrusions of midlatitude air into the vortex. The model was initialized with air parcels (APs) covering the northern Hemisphere in the potential temperature (θ) range between 350 and 1400 K. The horizontal resolution was 80 km and the vertical resolution 320 m, the latter being determined by the constant aspect ratio $\alpha = 250$ [*Konopka et al.*, 2004b]. The horizontal (isentropic) winds were interpolated from ECMWF data with a horizontal resolution of 1.125°, and the cross-isentropic velocities of the APs were calculated with a radiation module [*Zhong and Haigh*, 1995; *Morcrette*, 1991; *Konopka et al.*, 2004b]. The wind data were interpolated from the ECMWF pressure levels to 27 irregularly spaced isentropic levels between 300 and 2000 K. We used 25 K intervals between 400 and 600 K, rising to 100 K intervals above 800 K, and 50 K intervals elsewhere. Model runs of CLaMS using Met Office data (not shown) showed a difference of 10 to 20 K in the total descent of the vortex air during the winter (1 December 1999 to the beginning of March 2000), compared to ECMWF data [*Konopka et al.*, 2004b]. The cause of these different descents are different temperature data; temperature discrepancies between the Met Office and ECMWF data are discussed for winter 1999–2000 by *Manney et al.* [2003] and *Davies et al.* [2002]. Starting on 1 December 1999, an artificial, passive tracer was initialized with values of 100% inside and 0% outside the vortex. For the purpose of initialization, the edge of the polar vortex was calculated according to the *Nash et al.* [1996] criterion, which defines the vortex edge as the location of the strongest PV gradients with respect to equivalent latitude constrained by the proximity of the maximum wind velocity in the polar jet.

[11] Figures 3a–3c show the evolution of the artificial tracer from 1 December 1999 to 20 March 2000, averaged over the area of the vortex that was defined by three different criteria of the vortex edge. In particular, in Figure 3a the Nash criterion was employed for every day and each isentropic level. The vertical gray lines mark dates with minor warming events, as described in the previous section.

[12] Figure 3a shows three major dilution features: layerwise intrusions beginning at about 550 K, at about 1200 K, and at 1300 K (with dilution noticeable as yellow, green, and blue), and the vortex bottom at about 420 K. The vortex bottom appears as a sharp border below 420 K and descends slowly in the course of the winter. Near 550 K, the dilution of the tracer indicates an intrusion layer starting in the first

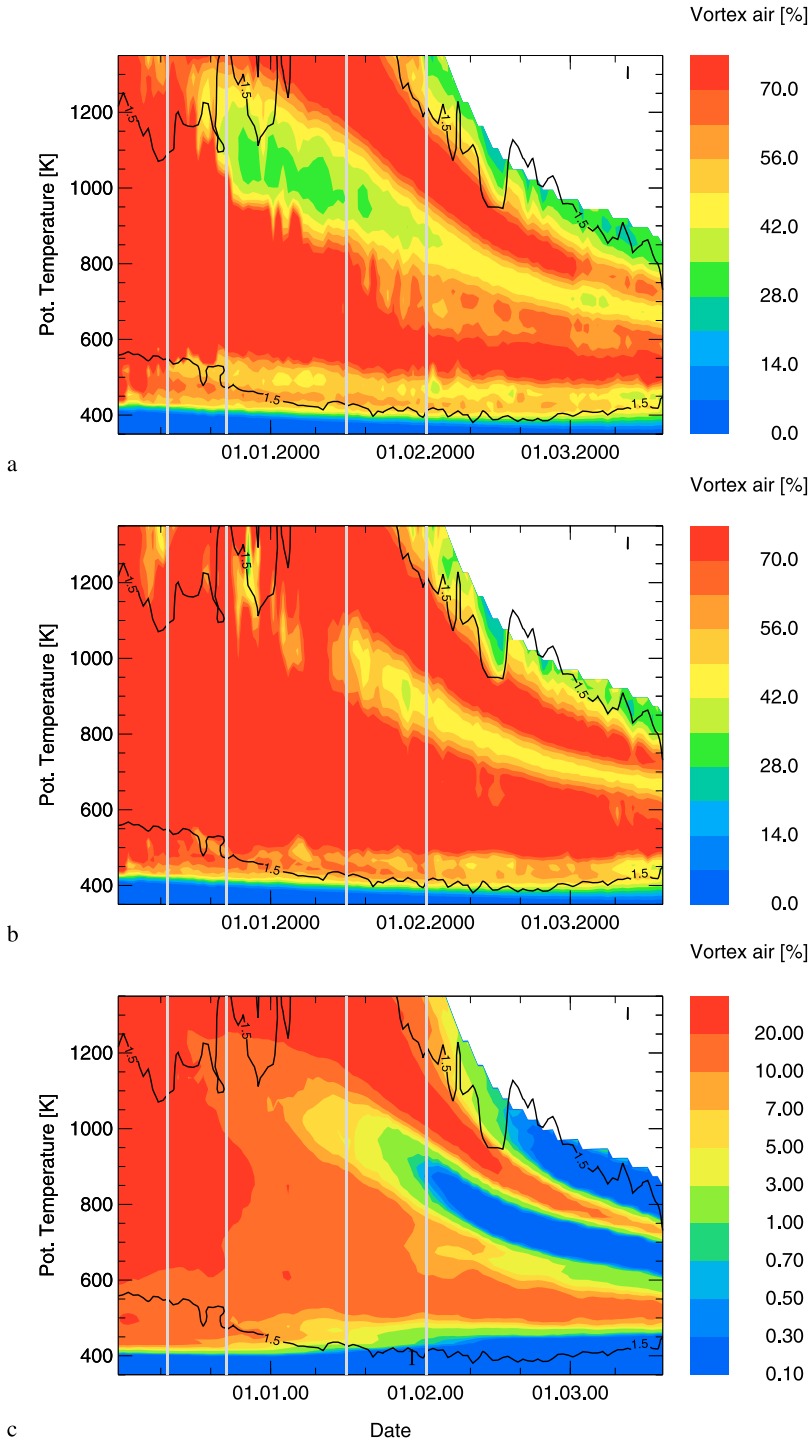

Figure 3. Vortex exemplified by three definitions of the vortex air parcels (APs). (a) Vortex APs [*Nash et al.*, 1996] criterion. (b) Inner vortex APs [*Tuck et al.*, 2002; *Chan et al.*, 1989]. (c) Relative contribution of "pure" vortex APs to the total number of APs northward of 30°N [*Konopka et al.*, 2005]. For detailed definitions see text. The black line denotes the contour of the maximum of the gradient of the modified PV = 1.5 PVU deg^{-1}, with MPV values greater than this threshold inside this contour. The vertical gray lines mark the dates of minor warming or wave amplification events reported by *Manney and Sabutis* [2000] and *Sabutis and Manney* [2000] occurring on 11 and 23 December 1999 and 16 January 2000, together with an additional warming event on 1 February 2000.

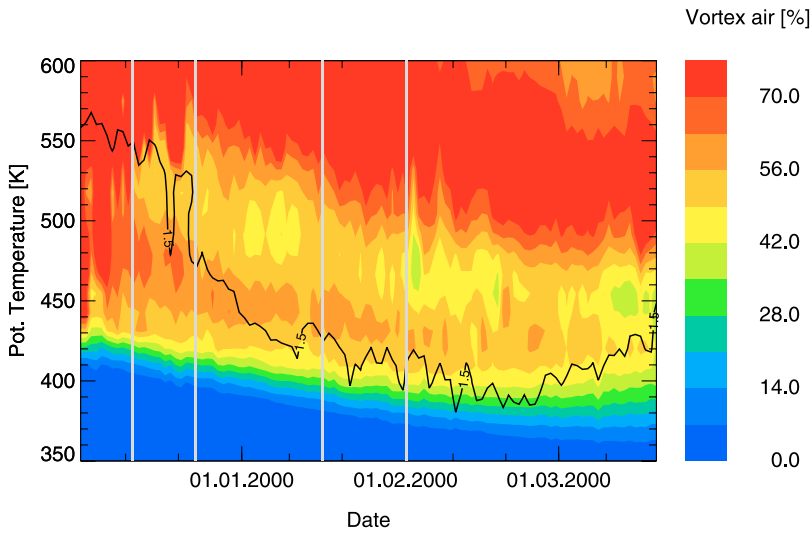

Figure 4. Vortex dilution in the lower part of the vortex as defined by the *Nash et al.* [1996] criterion. This figure displays a zoom into the lower part of Figure 3a.

days of December 1999. This altitude band is of greatest interest regarding ozone in the debate about exchange across the vortex edge because most of the ozone column resides and the associated loss occurs between 350 to 500 K. Furthermore, this is the region where aircraft data with high resolution are available. Therefore Figure 4 displays a zoom into the lowermost layers of Figure 3a. Using high-resolution aircraft tracer measurements from January to March 2000, *Jost et al.* [2002] detected that during this period, mixing into the polar vortex occurred preferentially at potential temperature levels of 450 K, 410 K, and 380 K. In Figure 4, between January and March we see enhanced dilution around the 450 K potential temperature level (this dilution feature starts at 550 K in December 1999). In March, the vortex bottom is located around 410 K. We cannot separate any distinct dilution layer below this altitude, probably since mixing in the model is still too strong. It is worth mentioning in this context that the altitude of the vortex bottom results from the initialization condition: on 1 December 1999 only those air parcels were labeled as vortex air which exceeded a given threshold of potential vorticity. If a transport barrier was established later in the winter, we would not be able to see it in our results. Actually, in December 1999 the lower stratospheric vortex strengthened rapidly, the maximum PV gradients only reaching average values after early January 2000 [*Manney and Sabutis*, 2000].

[13] A significant intrusion of midlatitude air into the vortex begins in December above 1300 K (Figure 3) and strengthens about mid-December near 1200 K. This intrusion is subject to diabatic descent, reaching 650 K in mid-March. The descent rates derived from CLaMS trajectories are in the same range as the experimental results of *Greenblatt et al.* [2002] and the long-term model studies of *Rosenfield and Schoeberl* [2001] (see Figure 2 of *Konopka et al.* [2004b] and the associated discussion). The strongest descent occurred during December and January at greater altitudes, with some mesospheric air reaching the 450 K isentropic surface by March [*Ray et al.*, 2002; *Plumb et al.*, 2002]. Consequently, information on air masses from altitudes above the model's upper boundary is required to simulate such behavior. To account for this, an update of the tracer value of the air parcels was made in the top layer of CLaMS after each model time step (1 day). According to the value of the potential vorticity, the air parcels were classified as part of the polar vortex or the midlatitudes. The artificial tracer in the top layer of the model was initialized with values of 100% (vortex) or 0% (out of vortex), without any intermediate values. The vortex edge in the top layer of CLaMS was defined for the whole model run at a constant PV value (26.9 PVU, modified after *Lait* [1994]) as proposed, for instance, by *Waugh et al.* [1999], who defined the polar vortex for 19 years with an adjusted threshold value of potential vorticity. Because we use relatively simple assumptions for the upper boundary update, in Figure 3 the three highest model layers were omitted and the upper right-hand corner is intentionally left white (to avoid misleading interpretation).

[14] In the first days of February, another intrusion appears above 1300 K. To some extent, these major dilution features correlate with planetary wave activities (see Figures 1 and 3). In Figure 3b, the definition of the vortex edge is based mainly on the properties of the wind velocity field. We divide the already defined polar vortex [*Nash et al.*, 1996] into an outer and inner vortex area with the inner vortex characterized by wind speed below 30 m s^{-1}. This definition is derived directly from meteorological observations in the altitude range from 350 to 500 K, obtained by ER-2 aircraft measurements [*Tuck et al.*, 2002; *Chan et al.*, 1989]. Restricting the analysis to the inner vortex APs, the dilution of the vortex (Figure 3b) shows the same pattern as discussed above (Figure 3a), although the dilution in the inner vortex region is in general smaller.

[15] A further possibility of studying the dilution and mixing of vortex APs without an explicit definition of the vortex edge is the study of the contribution of "pure" vortex APs relative to the total number of APs in a given region (here poleward of 30°N) derived directly from the model [*Konopka et al.*, 2005]. In this setup, the Nash criterion was only applied for the initialization procedure

to determine the vortex APs on 1 December 1999. The APs with a percentage of more than 80% vortex air are considered as ''pure'' vortex APs (Figure 3c). In contrast to Figures 3a and 3b, the contours in Figure 3c are logarithmically scaled.

[16] This kind of diagnostic shows similar features to the results presented in Figures 3a and 3b. We conclude that the derived pattern of mixing does not depend on the specific definition of the vortex edge: The results of all dilution studies show the same basic features. However, even if the pattern of mixing does not depend explicitly on the vortex definition, the quantification of mixing does of course depend on this definition. Therefore we would like to emphasize that in this study, we confine ourselves to the discussion of the conditions for weak or strong permeability of the vortex edge to intrusions into the vortex and do not intend to quantify the mass fluxes across the edge.

[17] Despite the temporal coincidence of the intrusions with increased wave activity spanning a vertical potential temperature range of several hundred Kelvin (Figure 1), wave activity alone cannot satisfactorily explain the observed, layer-wise intrusions that are amplified abruptly at particular altitudes. Intrusions into the vortex frequently seem to possess a shallow vertical structure [*Plumb et al.*, 1994; *Schoeberl and Newman*, 1995].

[18] The greatest day-to-day fluctuations of the EP flux divergence over the winter were found at above 1400 K (not shown), which is above the upper boundary of our model runs. This might explain the fact that two of the observed intrusions begin at the upper boundary level of the model data. With backward trajectory calculations, we found that the disturbed layers were exposed to increased wave activity (convergence) some days before the intrusion. However, high values of the EP flux divergence were also observed on other days without any significant influence being noticeable on the strength of the vortex edge and ordinary wave activity (Figure 2, right panel). Even similar patterns of EP flux divergence do not have similar effects on the strength of the vortex edge. Thus, considering only the EP flux, the relationship between the EP flux divergences and the intrusions into the vortex is apparently too indirect to explain the observed patterns of dilution.

4. Variability of the Vortex Edge

[19] The analysis of the vortex edge, calculated using the Nash criterion, shows variations of the edge of up to 20° of equivalent latitude from day to day, making the vortex area smaller or greater. Even *Chan et al.* [1989], defining the inner vortex (as described in the previous section) lying poleward of the polar jet, note that the boundary of the inner vortex is not stationary on different days, due to the variation of the wind maximum. Variations of the inner vortex of up to 10° in latitude in 4 days were documented for the Antarctic vortex in winter 1987, in an altitude range of 425 to 475 K potential temperature [*Chan et al.*, 1989]. In particular, on 2 days (from their sample of 12 days) the jet core was not identifiable, so the vortex boundary could not be determined [see *Chan et al.*, 1989, Figures 7b and 7k].

[20] However, the Nash criterion also requires knowledge of the location of the maximum of the wind jet. The vortex edge is defined as the location of the highest PV gradient on equivalent latitudes, constrained by the proximity of the polar jet, and both distributions will have strong peaks at the true vortex edge [*Nash et al.*, 1996]. *Nash et al.* [1996] used 15.2 m s^{-1} as an empirically determined limit below which the vortex edge could not be defined. This precondition is fulfilled in our study for all days and all altitudes. Comparing three diagnostics (Nash criterion, the area within PV contours, the area within contours of zonal winds), *Waugh et al.* [1999] studied the breakup criteria of the polar vortices for 19 years and found in general good agreement between them. *Manney et al.* [1994a] discuss the difficulties of defining the polar vortex due to strong spurious gradients caused by noise at high PV values and define preconditions for the existence of the polar vortex. Testing some of these criteria for winter 1999–2000 does not indicate much difference from the application of the Nash criterion.

[21] Figure 5 shows the distribution of the wind speed and of the gradient of modified PV [*Lait*, 1994] (MPV) with respect to equivalent latitude for several days between 1 December 1999 and 20 March 2000 for two levels of potential temperature. Following *Nash et al.* [1996], we first determined the distribution of PV and wind on equivalent latitudes and then we searched for the maxima. On the 600 K level for all days the wind speed and the gradient of PV show an explicit maximum at about 60–70° equivalent latitude, similar to the conditions shown in Figure 1 of *Nash et al.* [1996]. In contrast, on the 1300 K level, we see day-to-day variations of the intensity and location of the peaks. For the upper stratosphere, *Manney and Sabutis* [2000] also report highly variable gradients of PV and wind speed, explained by a double jet. Only some days in January show the expected maximum. Mainly at the beginning and around the end of the winter, the location of the maxima varies between the midlatitudes and the North Pole. Consequently, we restrict the possible range for the maximum of the gradient of PV to equivalent latitudes between 45°N and 72°N. The restriction to this equivalent latitude range in fact draws a distinction between those cases with a double-peaked jet and the situation with a single jet, which in general lies in this range. If there is a double-peaked jet, the Nash criterion finds, in general, a very broad or very small vortex, and the vortex edge often jumps between these two peaks from one day to the next. It was observed that intrusions into the vortex often begin under such conditions, suggesting weakening of the vortex edge in the case of a double-peaked jet.

[22] Figure 6 shows the day-to-day evolution of the maximum of the gradient of modified PV [*Lait*, 1994], hereinafter referred to as ∇MPV. Between 600 and 800 K the maximum gradient of MPV was strong throughout the winter. Below 550 and above 1000 K the intensity of the maximum of ∇MPV varies considerably, showing regions without an explicit maximum, and indicating only very weak gradients of MPV. However, it should be noted that weak gradients of MPV do not necessarily imply a weak transport barrier along the entire equivalent latitude contour; see, for example, the MPV field of Figure 7. Rather, we expect that along such a contour, segments with stronger gradients alternate with segments characterized by weaker gradients, i.e., enhanced permeability. Studying intrusions into the Arctic polar vortex of winter 1991–1992, *Plumb et*

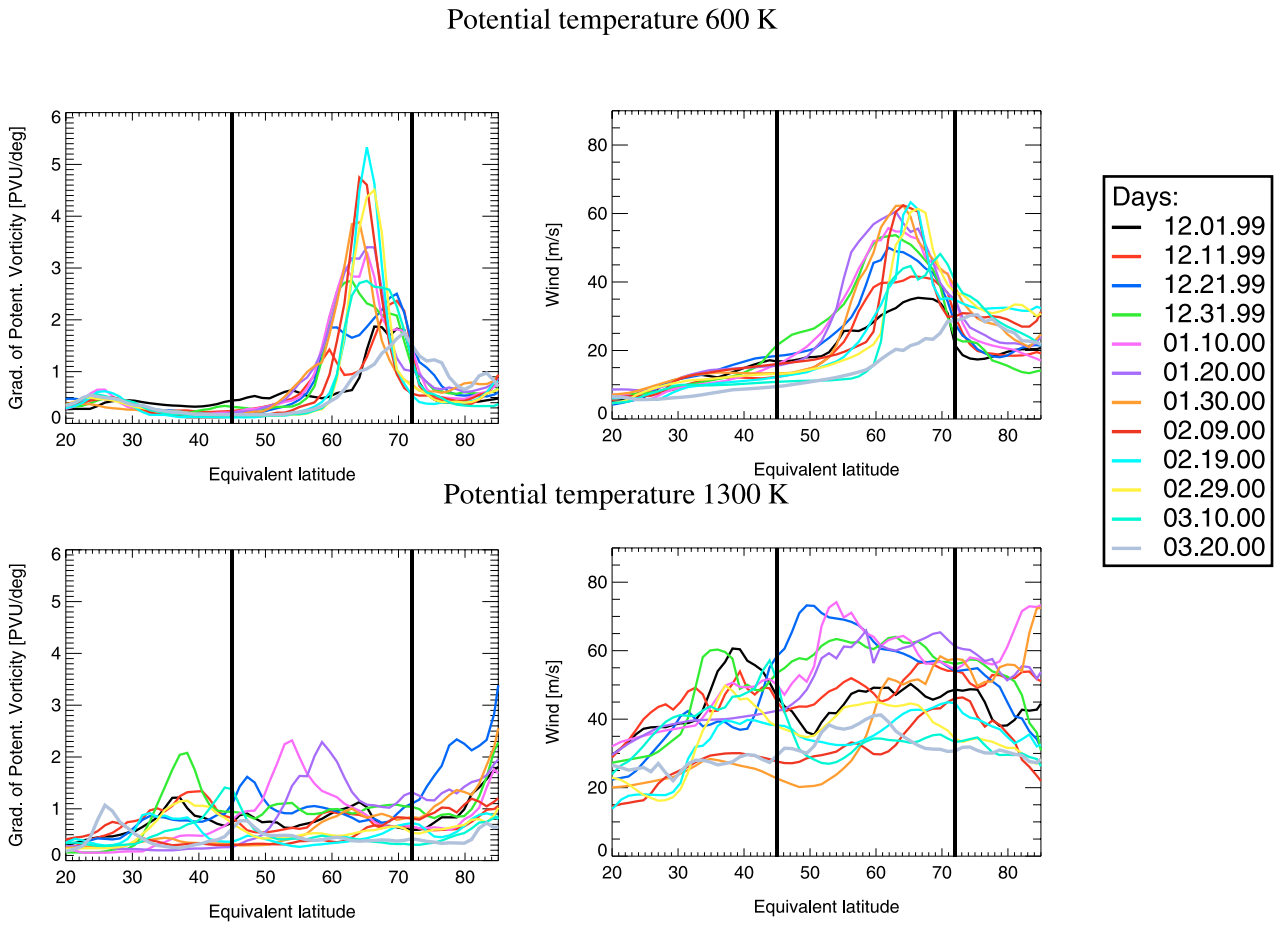

Figure 5. (left) Gradient of modified potential vorticity [*Lait*, 1994] and (right) wind speed of several days (colored lines) of winter 1999–2000. The two vertical lines mark the range of equivalent latitude where the vortex edge is expected.

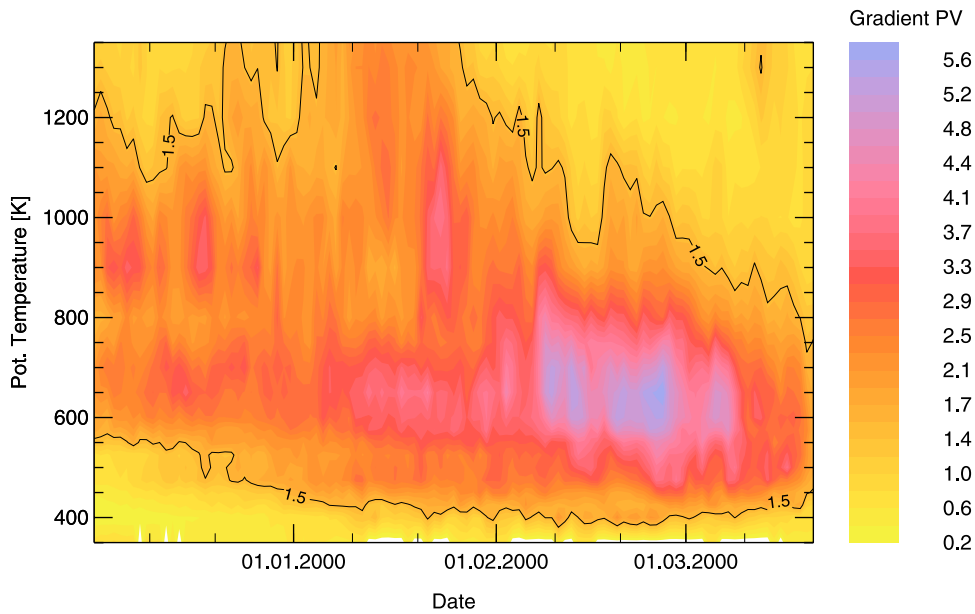

Figure 6. Maximum gradient of modified potential vorticity [*Lait*, 1994] in the range of 45° to 72° equivalent latitude. The black line is the contour of ∇MPV = 1.5 PVU deg^{-1}.

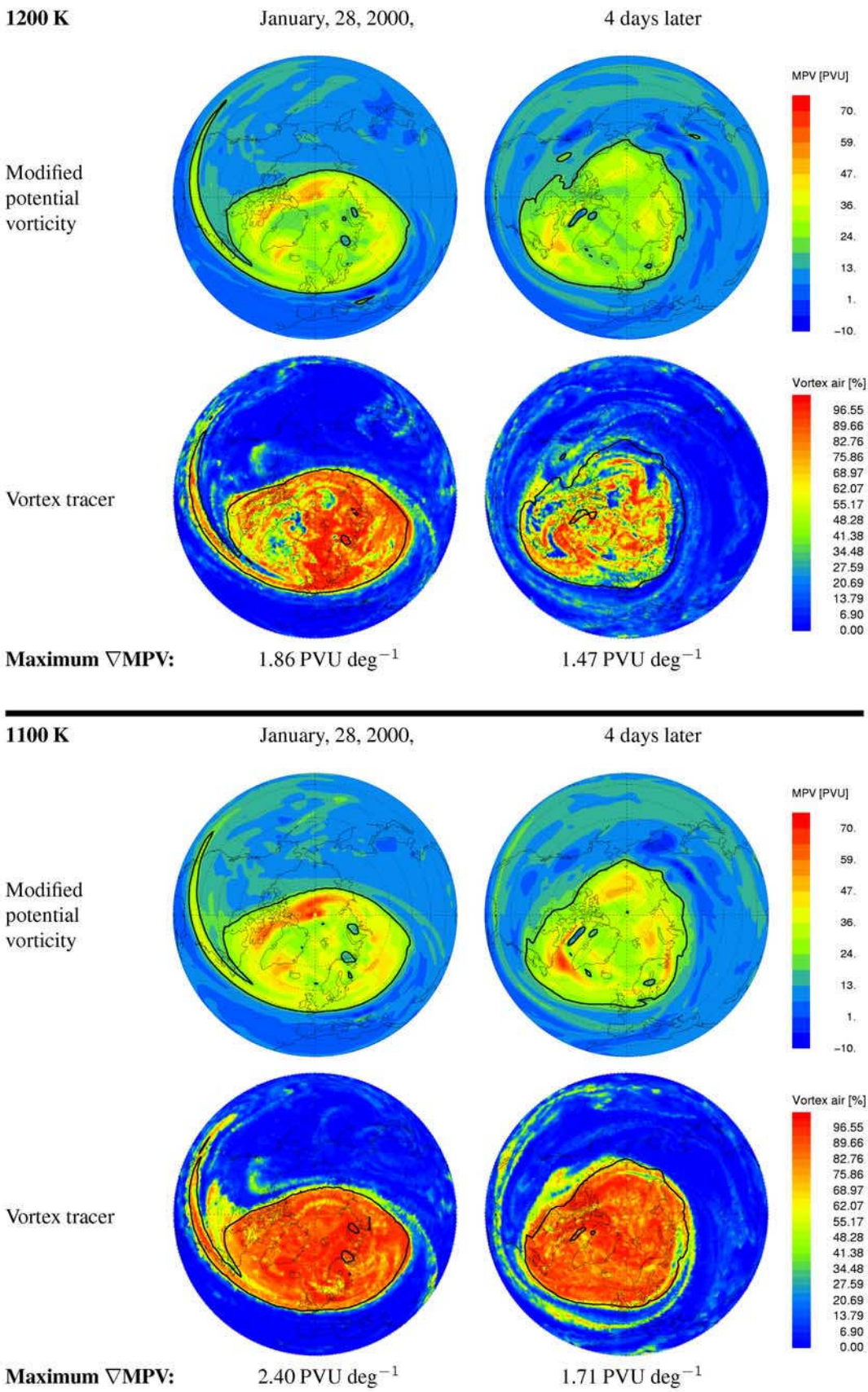

Figure 7. Evolution of the polar vortex (modified potential vorticity [*Lait*, 1994] and vortex tracer) from (left) 28 January 2000 to (right) 1 February 2000, for the potential temperature levels 1200 and 1100 K. The black contour indicates the vortex edge defined by the *Nash et al.* [1996] criterion.

al. [1994] notice difficulties in defining the vortex edge during such disturbed conditions. They describe the vortex edge as sharp in many places, but not continuously so, especially in regions of intrusion or extrusion.

[23] If there is no pronounced maximum of ∇MPV, the underlying assumption of the Nash criterion (strong PV gradient) is not fulfilled and, consequently, it is difficult to uniquely define an edge of the vortex. In such cases the "apparent edge" may vary considerably from one day to the next, leading to spurious intrusions into the vortex being diagnosed. If the wind speed shows a double peak, as was documented by *Manney and Sabutis* [2000] for the early 1999–2000 vortex in the upper stratosphere, the apparent vortex edge can suddenly "jump" from one wind peak to another.

[24] During a period with enhanced wave activity, we compared, the evolution of the polar vortex from an initially mostly undisturbed state to a highly diluted situation for a sample of vertically adjacent isentropes and several wave events. Figure 7 exemplifies the evolution of the polar vortex (MPV and vortex tracer) during a period of enhanced wave activity from 28 January 2000 to 1 February 2000 for two adjacent isentropes: 1200 K (upper panels) and 1100 K (bottom panels). The deformation of the vortex shape and its filamentation resembles the examples of wave breaking given by *Schoeberl and Newman* [1995] and *Dritschel and Saravanan* [1994]. Compare, for example, Figure 7 with Figure 1 of *Schoeberl and Newman* [1995] showing upper level wave breaking. Of all the studied vortex properties (wind speed, PV field, area of the vortex, ∇MPV), the maximum of ∇MPV shows the best correlation to the dilution of the vortex tracer, indicating increased mixing of midlatitude air parcels into the polar vortex during periods of weak maxima of ∇MPV. Figure 7 illustrates the progressive dilution of the vortex tracer at the 1200 K level from 28 January to 1 February 2000 (top panels), in contrast to the largely undisturbed situation at 1100 K (bottom panels). Though both levels show similar wave activity and vortex deformation, at 1100 K, the vortex edge was almost impermeable until 1 February 2000, while by this time the vortex air looks patchy at 1200 K, with massive intrusions of midlatitude air parcels. The maximum of ∇MPV values at 1100 K is higher than at the 1200 K, where it drops on 1 February 2000 below the value of 1.5 PVU deg^{-1}.

[25] It seems possible to characterize the permeability of the vortex edge, deduced using the Nash criterion, to intrusions into the vortex by defining a threshold value for the maximum of ∇MPV, which characterizes a "sufficiently impermeable" vortex edge, i.e., a transport barrier. *Manney et al.* [1994a] used such a criterion, namely the maximum average daily PV gradient as a diagnostic for the lifetime of the polar vortex.

[26] We determined the best value of this threshold empirically by comparing the behavior of the maximum of ∇MPV for isentropes and periods when midlatitude air parcels succeeded in crossing the vortex edge into the vortex with those cases when the vortex edge was largely impermeable. The threshold value of the maximum of ∇MPV, valid for winter 1999–2000, was found to be 1.5 PVU deg^{-1}. Therefore the contour of ∇MPV = 1.5 PVU deg^{-1} (meaning PV units per degree equivalent latitude) is drawn in Figure 6, as well as in Figure 3, to indicate the "sufficiently impermeable" vortex edge. If the maximum of ∇MPV is less than this threshold, we do not assume that mixing into the vortex occurs across the whole contour, but rather locally in some segments with weak gradients.

[27] The results of wave breaking studies show that in most cases, the forcing of breaking Rossby waves deforms the polar vortex, pulling out filaments of vortex air to the midlatitudes [e.g., *Polvani and Plumb*, 1992; *Dritschel and Saravanan*, 1994]. Only in more active situations can extra-vortex air be entrained into the vortex [*Polvani and Plumb*, 1992]. It is expected that such active phases will influence MPV and the steepness of its gradient, too. Thus, defining a "sufficiently impermeable" vortex edge by the maximum of ∇MPV, accounting for the dilution of the vortex, connects the resulting intrusions to the original wave activity. Analyzing the behavior of breaking waves, *Nakamura* [2004] distinguishes between inward (into the polar vortex) and outward (equatorward) wave breaking, detecting predominantly outward breaking waves. Accounting for these findings, it is consistent that although enhanced wave activity was observed, as seen in Figure 1, only in a few cases did inward breaking of the waves occur, leading to the diagnosed intrusions into the vortex.

[28] Considering the maximum of ∇MPV as a measure of the permeability of the polar vortex, we can explain the vortex dilution by a weak vortex edge with intrusions into the vortex beginning in regions of weak gradients of MPV; that means under conditions where the underlying assumptions of Nash criterion are de facto not fulfilled. Under such conditions, mixing of midlatitude air parcels into the vortex occurs and the otherwise quite isolated vortex preserves the mixed air parcels from December to spring, subjecting them to diabatic descent, as can be seen in Figure 3. Consequently, it seems reasonable in studies of mixing across the vortex to also check the value of the maximum gradient of PV. Further studies with data from winter 2002–2003 (not shown) confirm these observations.

5. Conclusions

[29] The analysis of the polar vortex in winter 1999–2000 indicates a complex, layered vertical structure of the vortex with layers consisting mostly of vortex air alternating with a few more diluted layers. At about the end of March 2000, the vertical structure of the vortex consists of well-isolated, pure vortex layers around 500 K and 750 K and some diluted layers in between and at the vortex bottom. Even such a cold Arctic vortex as that in 1999–2000 was not completely isolated from midlatitudes. Especially during December 1999, some air parcels from midlatitudes were mixed into the vortex, where they remained until the vortex breakup in spring. The diagnosed dilution patterns of the vortex do not depend explicitly on the definition of the vortex edge. The results of the studies using different definitions of the vortex edge show the same patterns. However, this is an example of a deep, cold polar vortex, with a mostly strong vortex edge. The application of this threshold to the data of winter 2002–2003 (not shown in this paper), which is characterized by an unusually cold period in December, but later showed much more wave

activity than winter 1999–2000 (major warmings, splitting of the vortex), supports the results presented here.

[30] The value of the EP flux divergence did not allow a differentiation between the disturbances where mixing into the vortex occurs and disturbances without intrusions. More promising results were obtained by the analysis of the maximum of the gradient of MPV, with respect to equivalent latitude. On some days and levels, MPV showed only weak gradients, without a clear maximum. In this case, the underlying assumption of the *Nash et al.* [1996] criterion (strong gradient) is not fulfilled and the determined "edge" does not constitute a transport barrier. In these cases we found intrusions into the vortex during winter 1999–2000 in our model results. Therefore it seems that mixing into the vortex is coupled to the steepness of maximum of the gradient of MPV. We conclude that by using the Nash criterion, the steepness of the maximum of MPV gradient should be considered, with an empirical threshold value of 1.5 PVU deg^{-1} suggested here, which is deduced on the basis of our study of winter 1999–2000. If this condition is valid, then the vortex edge should be considered as a largely impermeable barrier to transport into the vortex.

[31] **Acknowledgments.** We thank the European Centre for Medium-Range Weather Forecasts (ECMWF) for meteorological data support. The authors thank J. Oberheide for helpful contributions to the calculation of the Eliassen-Palm flux divergence and E. Nash for providing the code for the calculation of a criterion for the vortex edge. The authors gratefully acknowledge two reviewers for helpful comments on earlier versions of this paper.

References

Abrams, M. C., et al. (1996), ATMOS/ATLAS-3 observations of long-lived tracers and descent in the Antarctic vortex in November 1994, *Geophys. Res. Lett.*, *23*, 2341–2344.

Andrews, D. G., J. R. Holton, and C. B. Leovy (1987), *Middle Atmosphere Dynamics*, Elsevier, New York.

Bradshaw, N. G., G. Vaughan, and G. Ancellet (2002a), Generation of layering in the lower stratosphere by a breaking Rossby wave, *J. Geophys. Res.*, *107*(D2), 4011, doi:10.1029/2001JD000432.

Bradshaw, N. G., G. Vaughan, R. Busen, S. Garcelon, R. Jones, T. Gardiner, and J. Hacker (2002b), Tracer filamentation generated by small-scale Rossby wave breaking in the lower stratosphere, *J. Geophys. Res.*, *107*(D23), 4689, doi:10.1029/2002JD002086.

Butchart, N., and E. E. Remsberg (1986), The area of the stratospheric polar vortex as a diagnostic for tracer transport on an isentropic surface, *J. Atmos. Sci.*, *43*, 1319–1339.

Chan, K. R., S. G. Scott, T. P. Bui, S. W. Bowen, and J. Day (1989), Temperature and Horizontal Wind Measurements on the ER-2 Aircraft During the 1987 Airborne Antarctic Ozone Experiment, *J. Geophys. Res.*, *94*(D9), 11,573–11,587.

Chen, P. (1994), The permeability of the Antarctic vortex edge, *J. Geophys. Res.*, *99*(D10), 20,563–20,571.

Dahlberg, S. P., and K. P. Bowman (1994), Climatology of large-scale isentropic mixing in the Arctic winter stratosphere from analyzed winds, *J. Geophys. Res.*, *99*(D10), 20,585–20,599.

Davies, S., et al. (2002), Modeling the effect of denitrification on Arctic ozone depletion during winter 1999/2000, *J. Geophys. Res.*, *107*, 8322, doi:10.1029/2001JD000445. [printed *108*(D5), 2003]

Dritschel, D. G., and R. Saravanan (1994), Three-dimensional quasi-geostrophic contour dynamics, with an application to stratospheric vortex dynamics, *Q. J. R. Meteorol. Soc.*, *120*, 1267–1297.

Greenblatt, J., et al. (2002), Tracer-based determination of vortex descent in the 1999/2000 arctic winter, *J. Geophys. Res.*, *107*(D20), 8279, doi:10.1029/2001JD000937.

Grooß, J.-U., and R. Müller (2003), The impact of mid-latitude intrusions into the polar vortex on ozone loss estimates, *Atmos. Chem. Phys.*, *3*, 395–402.

Jost, H.-J., et al. (2002), Mixing events revealed by anomalous tracer relationships in the arctic vortex during winter 1999/2000, *J. Geophys. Res.*, *107*(D24), 4795, doi:10.1029/2002JD002380.

Juckes, M., and M. McIntyre (1987), A high resolution, one-layer model of breaking planetary waves in the stratosphere, *Nature*, *328*, 590–596.

Kawa, S., R. Bevilacqua, J. Margitan, A. Douglass, M. Schoeberl, K. Hoppel, and B. Sen (2002), Interaction between dynamics and chemistry of ozone in the setup phase of the Northern Hemisphere polar vortex, *J. Geophys. Res.*, *107*, 8310, doi:10.1029/2001JD001527. [printed *108*(D5), 2003]

Konopka, P., et al. (2004), Mixing and ozone loss in the 1999–2000 arctic vortex: Simulations with the three-dimensional Chemical Lagrangian Model of the Stratosphere (CLaMS), *J. Geophys. Res.*, *109*, D02315, doi:10.1029/2003JD003792.

Konopka, P., J.-U. Grooß, H.-M. Steinhorst, and R. Müller (2005), Mixing and chemical ozone loss during and after the Antarctic polar vortex major warming in September 2002, *J. Atmos. Sci.*, in press.

Lait, L. R. (1994), An alternative form for potential vorticity, *J. Atmos. Sci.*, *51*, 1754–1759.

Manney, G. L., and J. L. Sabutis (2000), Development of the polar vortex in the 1999–2000 Arctic winter stratosphere, *Geophys. Res. Lett.*, *27*, 2589–2592.

Manney, G. L., R. W. Zurek, M. E. Gelman, A. J. Miller, and R. Nagatani (1994a), The anomalous Arctic lower stratospheric polar vortex of 1992–1993, *Geophys. Res. Lett.*, *21*, 2405–2408.

Manney, G. L., R. W. Zurek, A. O'Neill, and R. Swinbank (1994b), On the motion of air through the stratospheric polar vortex, *J. Atmos. Sci.*, *51*, 2973–2994.

Manney, G., L. Froidevaux, M. Santee, N. Livesey, J. Sabutis, and J. Waters (2003), Variability of ozone loss during Arctic winter (1991 to 2000) estimated from UARS Microwave Limb Sounder measurements, *J. Geophys. Res.*, *108*(D4), 4149, doi:10.1029/2002JD002634.

McIntyre, M. E. (1995), The stratospheric polar vortex and sub-vortex: Fluid dynamics and midlatitude ozone loss, *Philos. Trans. R. Soc. London, Ser. A*, *352*, 227–240.

McIntyre, M. E., and T. N. Palmer (1983), Breaking planetary waves in the stratosphere, *Nature*, *305*, 593–600.

McKenna, D. S., P. Konopka, J.-U. Grooß, G. Günther, R. Müller, R. Spang, D. Offermann, and Y. Orsolini (2002), A new Chemical Lagrangian Model of the Stratosphere (CLaMS): I. Formulation of advection and mixing, *J. Geophys. Res.*, *107*(D16), 4309, doi:10.1029/2000JD000114.

Morcrette, J.-J. (1991), Radiation and cloud radiative properties in the European Centre for Medium-Range Weather Forecasts forecasting system, *J. Geophys. Res.*, *96*(D5), 9121–9132.

Nakamura, N. (2004), Quantifying asymmetric wave breaking and two-way transport, *J. Atmos. Sci.*, *61*, 2735–2748.

Nash, E. R., P. A. Newman, J. E. Rosenfield, and M. R. Schoeberl (1996), An objective determination of the polar vortex using Ertel's potential vorticity, *J. Geophys. Res.*, *101*(D5), 9471–9478.

Newman, P., et al. (2002), An overview of the SOLVE-THESEO 2000 campaign, *J. Geophys. Res.*, *107*(D10), 8259, doi:10.1029/2001JD001303.

Oberheide, J. (2000), Messung und Modellierung von Gezeitenwellen in der mittleren Erdatmosphäre: Ergebnisse des CRISTA-Experiments, Ph.D. thesis, Bergische Univ. - Gesamthochschule Wuppertal, Germany.

Pawson, S., and T. Kubitz (1996), Climatology of planetary waves in the northern stratosphere, *J. Geophys. Res.*, *101*(D12), 16,987–16,996.

Pierce, R. B., and T. D. Fairlie (1993), Observational evidence of preferred flow regimes in the Northern Hemisphere winter stratosphere, *J. Atmos. Sci.*, *50*, 1936–1949.

Pierce, R. B., T. D. Fairlie, W. L. Grose, R. Swinbank, and A. O'Neill (1994), Mixing processes within the polar night jet, *J. Atmos. Sci.*, *20*, 2957–2972.

Plumb, R. A., D. W. Waugh, R. J. Atkinson, P. A. Newman, L. R. Lait, M. R. Schoeberl, E. V. Browell, A. J. Simmons, and M. Loewenstein (1994), Intrusions into the lower stratospheric Arctic vortex during the winter of 1991–1992, *J. Geophys. Res.*, *99*(D1), 1089–1105.

Plumb, R. A., W. Heres, J. L. Neu, N. M. Mahowald, J. del Corral, G. C. Toon, E. Ray, F. Moore, and A. E. Andrews (2002), Global tracer modeling during SOLVE: High latitude descent and mixing, *J. Geophys. Res.*, *107*, 8309, doi:10.1029/2001JD001023. [printed *108*(D5), 2003]

Polvani, L., and R. Plumb (1992), Rossby wave breaking, microbreaking, filamentation, and secondary vortex formation: The dynamics of a perturbed vortex, *J. Atmos. Sci.*, *49*, 462–476.

Randel, W. J., J. C. Gille, A. E. Roche, J. B. Kumer, J. L. Mergenthaler, J. W. Waters, E. F. Fishbein, and W. A. Lahoz (1993), Stratospheric transport from the tropics to middle latitudes by planetary-wave mixing, *Nature*, *365*, 533–535.

Rao, V. B., M. B. Rosa, J. P. Bonatti, and S. H. Franchito (2003), Stratospheric final warmings in the Southern Hemisphere and their energetics, *Meteorol. Atmos. Phys.*, *83*, doi:10.1007/s00703-002-0558-6.

Ray, E. A., F. L. Moore, J. W. Elkins, D. F. Hurst, P. A. Romashkin, G. S. Dutton, and D. W. Fahey (2002), Descent and mixing in the 1999–2000 northern polar vortex inferred from in situ tracer measurements, *J. Geophys. Res.*, *107*(D20), 8285, doi:10.1029/2001JD000961.

Rosenfield, J. E., and M. R. Schoeberl (2001), On the origin of polar vortex air, *J. Geophys. Res.*, *106*(D24), 33,485–33,497.

Rosenfield, J. E., P. A. Newman, and M. R. Schoeberl (1994), Computations of diabatic descent in the stratospheric polar vortex, *J. Geophys. Res.*, *99*(D8), 16,677–16,689.

Sabutis, J. L., and G. L. Manney (2000), Wave propagation in the 1999–2000 Arctic early winter stratosphere, *Geophys. Res. Lett.*, *27*, 3205–3208.

Schoeberl, M. R., and D. L. Hartmann (1991), The dynamics of the stratospheric polar vortex and its relation to springtime ozone depletions, *Science*, *251*, 46–52.

Schoeberl, M. R., and P. A. Newman (1995), A multiple-level trajectory analysis of vortex filaments, *J. Geophys. Res.*, *100*(D12), 25,801–25,815.

Tilmes, S., R. Müller, J.-U. Grooß, D. McKenna, J. Russell, and Y. Sasano (2003), Calculation of chemical ozone loss in the Arctic winter 1996–1997 using ozone-tracer correlations: Comparison of Improved Limb Atmospheric Spectrometer (ILAS) and Halogen Occultation Experiment (HALOE) results, *J. Geophys. Res.*, *108*(D2), 4045, doi:10.1029/2002JD002213.

Tuck, A. F., S. J. Hovde, E. C. Richard, D. W. Fahey, R. S. Gao, and T. P. Bui (2002), A scaling analysis of ER-2 data in the inner Arctic vortex during January–March 2000, *J. Geophys. Res.*, *107*, 8306, doi:10.1029/2001JD000879. [printed *108*(D5), 2003]

Waugh, D., and W. Randel (1999), Climatology of Arctic and Antarctic polar vortices using elliptical diagnostics, *J. Atmos. Sci.*, *56*, 1594–1613.

Waugh, D. W., W. J. Randel, S. Pawson, P. A. Newman, and E. R. Nash (1999), Persistence of the lower stratospheric polar vortices, *J. Geophys. Res.*, *104*(D22), 27,191–27,201.

Zhong, W., and J. D. Haigh (1995), Improved broadband emissivity parameterization for water vapor cooling rate calculations, *J. Atmos. Sci.*, *52*, 124–138.

G. Günther, P. Konopka, R. Müller, and H.-M. Steinhorst, Forschungszentrum Jülich, Institute for Stratospheric Chemistry (ICG-I), Research Center, 52425 Jülich, Germany. (h.steinhorst@fz-juelich.de; p.konopka@fz-juelich.de)